



Silencing proline-rich coiled-coil 2C inhibit the proliferation and metastasis of liver cancer cells

Kai Zhang¹, Jiaming Xu¹, Ran Chen²

¹Department of Oncology Surgery, Yuebei People's Hospital Affiliated to Shantou University Medical College, Shaoguan, China; ²Department of Gynaecology, Yuebei People's Hospital Affiliated to Shantou University Medical College, Shaoguan, China

Contributions: (I) Conception and design: K Zhang; (II) Administrative support: R Chen; (III) Provision of study materials or patients: K Zhang; (IV) Collection and assembly of data: J Xu; (V) Data analysis and interpretation: J Xu; (VI) Manuscript writing: All authors; (VII) Final approval of manuscript: All authors.

Correspondence to: Ran Chen. Yuebei People's Hospital Affiliated to Shantou University Medical College, Shaoguan 512000, China.

Email: 119827817@qq.com.

Background: Proline-rich coiled-coil 2C (*PRRC2C*) is located in the chromosome region 1q where hepatocellular carcinoma (HCC) frequently undergoes genomic fragment amplification, but its role in HCC is unknown. In this study, we aimed to explore the correlation of *PRRC2C* with HCC diagnosis and progression, as well as its influence on the biological behavior of HCC cells.

Methods: The Cancer Genome Atlas (TCGA) RNA-sequencing datasets of 371 cases of primary liver cancer and 50 normal liver tissue specimens were obtained to analyze correlation between *PRRC2C* expression and HCC staging, grades, and overall survival. After confirming expression of *PRRC2C* in HCC cells, *PRRC2C* silencing was performed. *Celigo* cell counting, cell clone formation, MTT (3-(4,5-dimethylthiazol-2-yl)-2,5-diphenyltetrazolium bromide) assay and Flow cytometry were used to detect the cell proliferation and apoptosis; wound healing and Transwell assays were used to detect the invasion abilities of cells. Xenograft transplantation in nude mice was performed to investigate the impact of *PRRC2C* knockdown on tumorigenic capabilities. In addition, the expression levels of EMT (epithelial-mesenchymal transition)-related genes, including E-cadherin, N-cadherin, *Twist1*, *Snail*, *Slug*, and *Smad2/3/4*, were detected.

Results: Analysis of TCGA data sets revealed that patients with high *PRRC2C* expression had significantly shorter overall survival. *PRRC2C* was abundantly expressed in four human hepatocarcinoma cell lines. After knockdown *PRRC2C*, the proliferation of HCC cells were suppressed and the numbers of apoptotic cells increased. Migration and invasion ability of HCC cells were inhibited by *PRRC2C* knockdown. Meanwhile, *PRRC2C* silencing inhibited the tumor formation (indicated by reduced tumor volume and weight compared to the control group) in BALB/c (Bagg Albino Laboratory-bred strain) nude mice. The expressions of EMT-related genes N-cadherin and Vimentin were significantly lower in the *PRRC2C* knockdown group than in the control group.

Conclusions: *PRRC2C* promotes the proliferation and metastasis of liver cancer cells and inhibited apoptosis, potentially through upregulation of EMT related N-cadherin and Vimentin.

Keywords: Apoptosis; hepatocellular; neoplasm metastasis; proliferation; *PRRC2C*

Submitted Dec 07, 2022. Accepted for publication Feb 10, 2023. Published online Feb 28, 2023.

doi: 10.21037/jgo-23-10

View this article at: <https://dx.doi.org/10.21037/jgo-23-10>

Introduction

Globally, the incidence and mortality of hepatocellular carcinoma (HCC) remain high. Up to 2018 (1), 841,000 new cases and 786,000 cases of liver cancer-related deaths, accounted for 8.2% of total cancer-related deaths, were reported worldwide. Due to the occult onset and high malignant degree, patients were often diagnosed at advanced stages and has less than 16% overall 5-year survival rate (2). However, the effective curable therapies only for early HCC, so poor prognosis remains a challenge that needs to be solved. Identification of specific tumor molecular markers may help earlier diagnosis, as well as further understanding of the molecular mechanism that mediates HCC tumorigenesis. In recent years, there have been a number of studies on molecular mechanisms of liver cancer, such as *FAM83D*, which promotes the proliferation and migration of hepatocellular carcinoma cells by inhibiting the *FBXW7/MCL1* pathway (3).

mRNA processing, transport, translation, and eventually degradation involve a large variety of dedicated protein complexes that commonly assemble into large membraneless structures such as stress granules (SGs). *PRRC2C* is an important stress granules protein (4). Proline-rich coiled-coil 2C (*PRRC2C*, or *KLAA1096*) was highly expression in the adult spinal cord, followed by the adult liver, brain, lung, and ovary, and fetal liver and brain (5). It has been identified as cancer related gene. The gene is located in the chromosome region 1q23-24, which was frequently undergoes chromosomal gain in bladder tumors, and upregulation of this gene has been found to be associated with bladder tumor and invasive lesions (6).

Highlight box

Key findings

- knockdown of *PRRC2C* could inhibit the proliferation and induce apoptosis of human hepatocarcinoma cell lines while reducing tumorigenicity of HCC cells in nude mice.

What is known and what is new?

- *PRRC2C* is an important stress granules protein.
- *PRRC2C* promotes the proliferation and metastasis of liver cancer cells and inhibited apoptosis, potentially through upregulation of EMT related N-cadherin and Vimentin.

What is the implication, and what should change now?

- *PRRC2C* may be relevant to the occurrence and development of liver cancer and may be used as an intervention target.

In addition, alternative splicing of *PRRC2C* was suggested to be related with lung adenocarcinoma (7); and mutation of *PRRC2C* was reported to be associated with Endemic Burkitt lymphoma (8). The expression of *PRRC2C* protein showed a tendency to be present in Serum of preeclampsia patients (9). The similar chromosome region has been reported to have frequent amplification in HCC (10), however the involvement and function of *PRRC2C* have not been explored in HCC. Therefore, we analyzed its correlation with HCC by screening TCGA database in this study and the functions of *PRRC2C* in HCC cell behaviors were explored in cellular experiments and xenograft animal models. We present the following article in accordance with the ARRIVE reporting checklist (available at <https://jgo.amegroups.com/article/view/10.21037/jgo-23-10/rc>).

Methods

Cell culture

Four liver cancer cells (BEL-7402, BEL-7404, SMMC-7721, and Hep G2) were purchased from Shanghai Cell Bank of Chinese Academy of Sciences. The cells were supplemented with 100 mL/L FBS in 50 mL/L CO₂ at 37 °C in Dulbecco's Modified Eagle's Medium (DMEM; Corning, Wu jiang, China).

The Cancer Genome Atlas data analysis

We analyzed the difference between *PRRC2C* mRNA levels in 371 liver cancer and 50 normal liver tissue using the TCGA database portal (<http://cancergenome.nih.gov/>), as well as *PRRC2C* among different Tumor Nodes Metastases (TNM) stage and pathological grades. The correlation between overall survival (OS) and the *PRRC2C* high or low expression also be analyzed by using Kaplan-Meier survival analysis. The study was conducted in accordance with the Declaration of Helsinki (as revised in 2013).

PRRC2C gene knockdown in BEL-7404 and SMMC-7721 cells

To silence *PRRC2C*, shRNA construct containing targeted siRNA oligo "5'-GCTGTATTATCTGGCTATT-3'" was synthesized by Genechem company (Shanghai, China) and cloned into GV115 plasmid vector (Genechem, shanghai, China). The plasmid was packed into lentivirus and transfected into cells using transfection reagents

Table 1 Primer sequences used for real-time PCR

Primer information	Upstream primer sequence	Downstream primer sequence
Reference GAPDH (glyceraldehyde-3-phosphate dehydrogenase)	TGACTTCAACAGCGACACCCA	CACCCTGTTGCTGTAGCCAAA
Target <i>PRRC2C</i> (proline-rich coiled-coil 2C)	CCATCAGTAGCAAAAGTTCCC	CTTCGCTCTTCCTTCCAG

PCR, polymerase chain reaction.

(Genechem, Shanghai, China) according to manufacturer's instructions. The efficiency of transfection was confirmed by detecting the fluorescence (introduced by eGFP gene in the plasmid vector) at 72-h after lentivirus infection.

RNA isolation and reverse transcription polymerase chain reaction (RT-PCR)

We used TRIZOL reagent (Pufei, Shanghai, China) to isolate total RNA from cell culture samples, and reverse transcriptions were performed by using the Promega M-MLV kit (Promega, Beijing, China). The real-time RT-PCR was performed using the SYBR Master Mix (Takara, Otsu, Japan) according to the manufacturer's instructions. Primers are listed in *Table 1*. The $2^{-\Delta\Delta C_t}$ method was used to calculate the relative mRNA expression.

Western blotting

In briefly, total protein was isolated from cells and concentration was determined using BCA assay. Equal amounts of proteins (20 μ g) were resolved by 10% SDS-PAGE and then transferred onto a polyvinylidene difluoride (PVDF) membrane (Millipore, Bedford, MA, USA). Before the membrane was incubated overnight at 4 °C with the primary antibody, we blocking protein for 1h with 5% non-fat milk, and then incubated with secondary antibodies. The primary antibodies used for western blotting as follows: N-cadherin Mouse Anti-Flag (1:2,000, Sigma, F1804), Mouse anti-GAPDH (1:2,000, Santa-Cruz sc-32233), anti-rabbit IgG antibody (1:5,000; Santa-Cruz, sc-2005).

Cell counts

Cells were seeded into 96-well plates with a density of 2,000 cells/well and cultured at 37 °C in a humidified atmosphere with 5% CO₂. After culturing 24 h, the number of cells were counted with a Celigo Image Cytometer (Nexcelom, Lawrence, MA USA). All experiments were repeated three times.

MTT assay

5 mg/mL 3-(4,5-dimethylthiazol-2-yl)-2,5-diphenyltetrazolium bromide (MTT, 20 μ L/well) was added to medium and the cells were incubated at 37 °C for 4–6 h, 100 μ L DMSO solution was added to each well and cells were incubated for another 5 min with constant shaking after aspirating the supernatant. The absorbance (A) at 490 nm was measured using a spectrophotometric plate reader (Thermo, USA, Nanodrop 2000) and cell growth curves were plotted.

Colony formation assays

Colony formation assays as previously described (11). sh*PRRC2C*-BEL-7404, sh*PRRC2C*-SMMC-7721, shCtrl-BEL-7404 and shCtrl-SMMC-7721 Cells (800 cells/well) were seeded in 6-well plates and cultured at 37 °C for 2 weeks. After 14 days, cell colonies were fixed with methanol and stained with 0.1% crystal violet (Sigma), and then visible colonies were manually counted under a microscope. The determination was carried out in triplicate.

Wound healing assay

Cells were seeded in 96-well plates at a density of 5×10^4 cells/well. When the cells formed a tight cell monolayer on the bottom of the plate, a sterilized tip was scraped across the cell monolayer. We washed the cells in PBS three times after remove the cell debris. Then to remove the complete DMEM and add serum-free DMEM into each well. Photomicrographs were taken by an IX71 inverted microscope (Olympus Corporation) at the scratch (0 h) and 24 h later. This assay was repeated 3 times.

Transwell assay

Cells inserts were coated without Matrigel (BD Bioscience). shCtrl-BEL-7404 and sh*PRRC2C*-BEL-7404 cells were seeded a density of 1×10^5 cells/well in DMEM without serum in the upper chamber. Then, 600 μ L DMEM

supplemented with 30% FBS was added to the lower chamber. After 16 h of incubation, a cotton swab was used to wipe the non-invasive cells. The invasive cells were fixed with 95% ethanol for 30 min at room temperature and stained with for 40 min at room temperature, followed by cellular count and photograph under a fluorescence microscope (Olympus Corporation, Tokyo, Japan) at a magnification of $\times 100$.

Flow cytometry detected cellular apoptosis

Cells were washed with cold PBS two time and then resuspended at a concentration of 10^6 cells/mL in $1 \times 300 \mu\text{L}$ Binding Buffer (BD Biosciences, USA). Subsequently, the cells were incubated with $5 \mu\text{L}$ Annexin V-FITC for 10 min followed by $5 \mu\text{L}$ propidium iodide (PI) at 37°C in darkness for 5 min. They were analyzed by flow cytometry (FACS calibur, BD Biosciences) within 1 h. The percentage of apoptotic cells in samples were determined by estimating the percentage of Annexin V+ PI+ and Annexin V+ PI- cells. This assay was conducted in triplicate.

Xenograft tumor model

5×10^6 cells in $200 \mu\text{L}$ DMEM were injected into the right cutaneous armpit of two groups of laboratory mice (4-week-old, female, BALB/c nude mice, 10 in each group, purchased from Shanghai Lingchang Biotechnology Co., LTD). Nude mice were housed in the SPF-grade Experimental Animal Center with a 12:12 light: dark cycle and access to food and water. Each mouse was kept in a cage alone. We measured laboratory mice weight, tumor length and short diameter of tumor after 15 days of injection and collected data 2 times a week for 3 weeks. Lumina LT In Vivo Imaging System (Perkin Elmer, US) was used to regularly visualize total fluorescence in the tumorous regions. All animals were sacrificed at 28 days and the tumors were isolated. The tumor tissue and liver of laboratory mice were collected and fixed in a 10% buffered formaldehyde solution; Tumor growth was monitored at regular intervals by measuring tumor diameter using a caliper. Tumor volume was determined by $(\text{length} \times \text{width}^2)/2$. This research was performed under a project license (No. SUMC2019-355) granted by the Medical Animal Care & Welfare Committee of Shantou University Medical College, in compliance with the Shantou University guidelines for the care and use of animals. A protocol was prepared before the study without registration.

Statistical analysis

Statistical analysis was performed using SPSS 23.0 (IBM, IL, USA) and GraphPad Prism 5 (GraphPad Software, CA, USA) softwares. Differences between two groups were explored using student's *t*-test. Non-normally distributed parameters were compared between groups using rank-sum test. Kaplan-Meier analysis for overall survival. Statistical analysis summary data are expressed as the means \pm standard deviation (SD). A P value <0.05 was considered significant.

Results

PRRC2C expression was correlated with hepatocarcinoma grades and survival

TCGA data analysis showed that the level of *PRRC2* mRNA in liver cancer samples ($n=371$) was upregulated compared to adjacent normal tissue samples ($n=50$) ($P<0.001$, *Figure 1A*). we observed that a statistically significant increase in *PRRC2C* expression level was correlated not only with the advanced TNM staging (*Figure 1B*) and poor pathological grading (*Figure 1C*). but also, with the shortened overall survival of patients (HR =1.47, 95% CI: 1.02–2.12, $P=0.039$) (*Figure 1D*).

Downregulation of PRRC2C inhibits cell proliferation and promote apoptosis of hepatocarcinoma cells

Real-time PCR analysis confirmed that *PRRC2C* was abundantly expressed in cultured human HCC cell lines (BEL-7402, BEL-7404, SMMC-7721, HepG2) (*Figure 1E*). We selected BEL-7404 and SMMC-7721 to explore the biological function of *PRRC2C*. Plasmids vectors containing shRNA sequences targeted to *PRRC2C* were successfully transfected into BEL-7404 and SMMC-7721 cells, and efficient silencing were 74.0% and 64.6%, respectively (*Figure 1F*). Further confirmation of a decrease in protein levels (*Figure 1G*).

Then, BEL-7404 cells were transfected with *PRRC2C* and negative control shRNA constructs. The results showed that *PRRC2C* knockdown significantly reduced viable cell number, cell proliferation, and colony formation compared to the negative control group. As shown in *Figure 2A-2C*. In addition, apoptosis analysis (*Figure 2D*) proved that *PRRC2C* knockdown resulted in an increase in the percentage of apoptotic cells (19.94% compared to 1.44% in the control group).

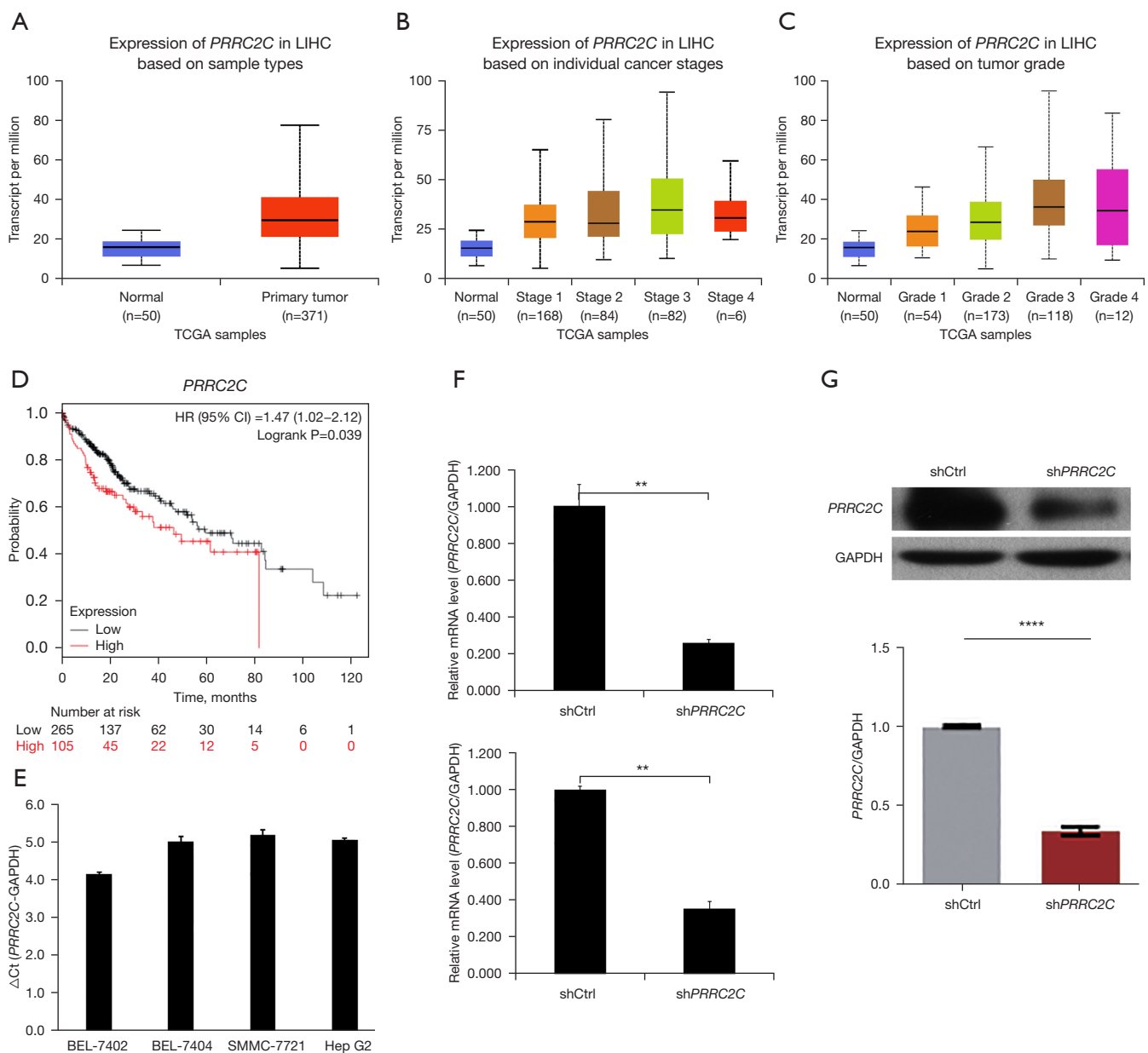
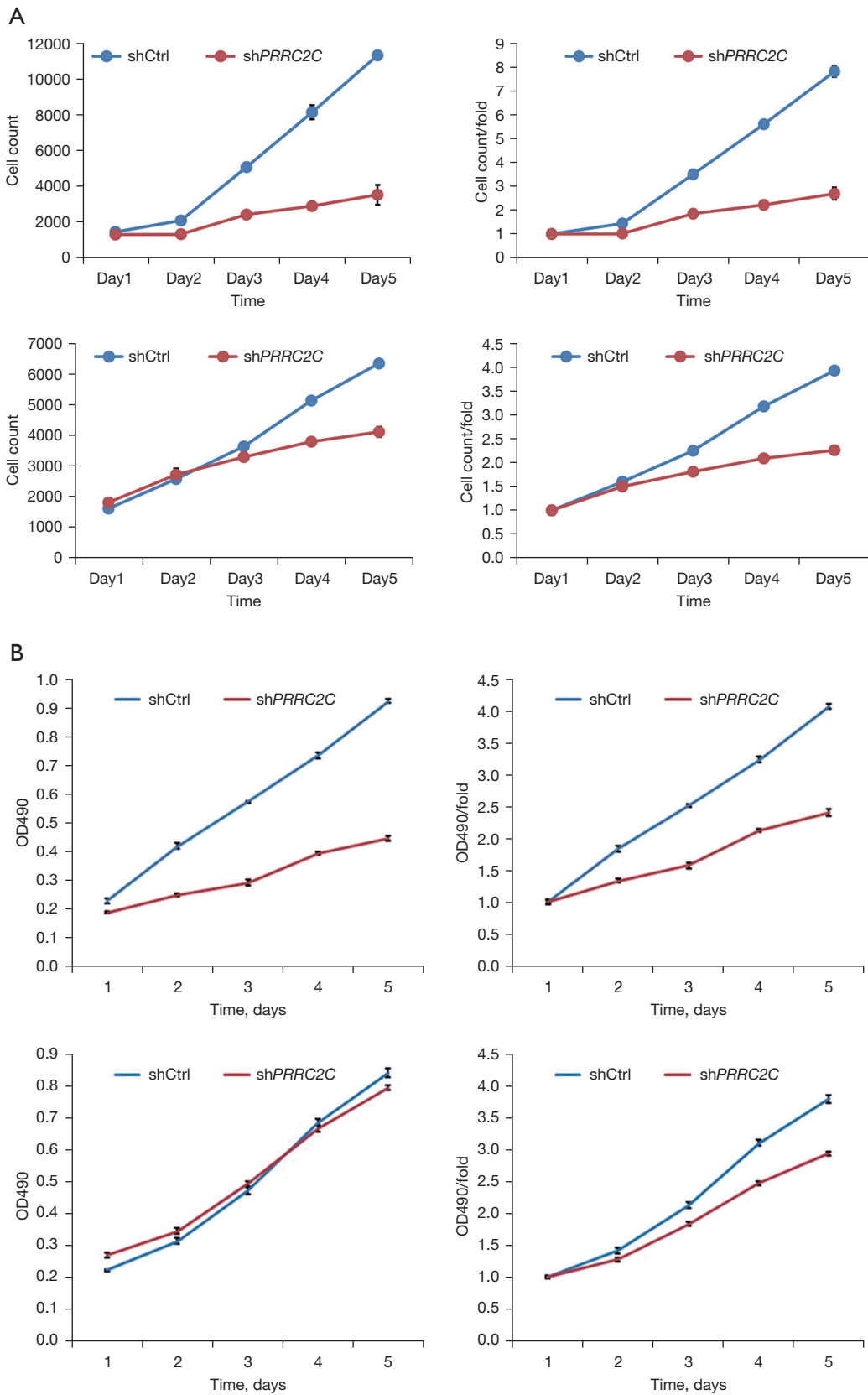
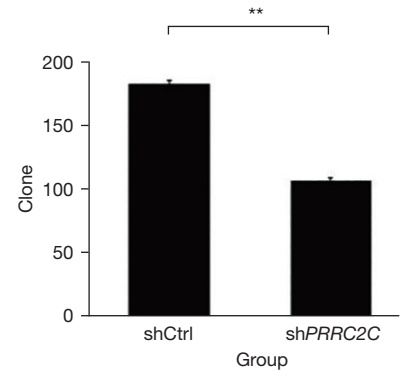
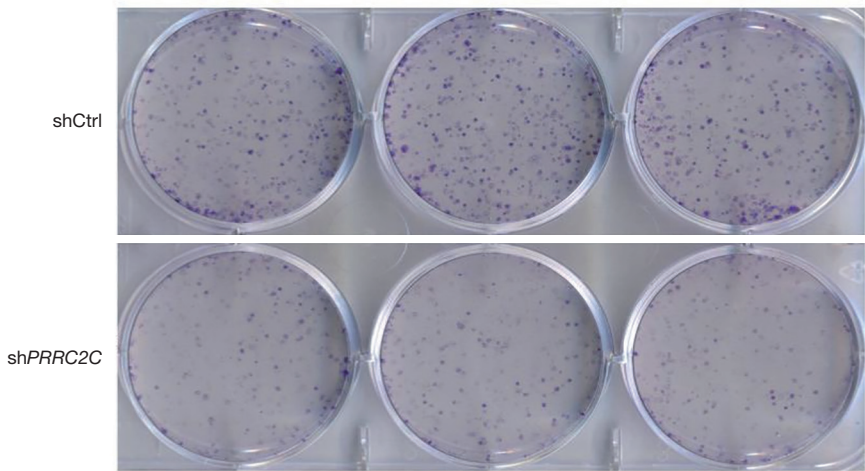
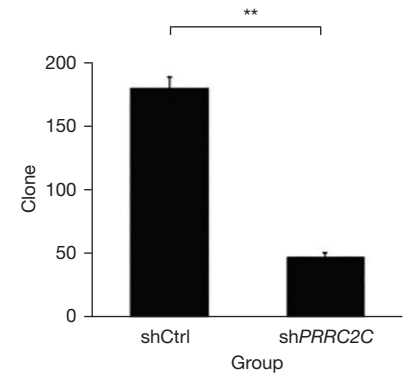
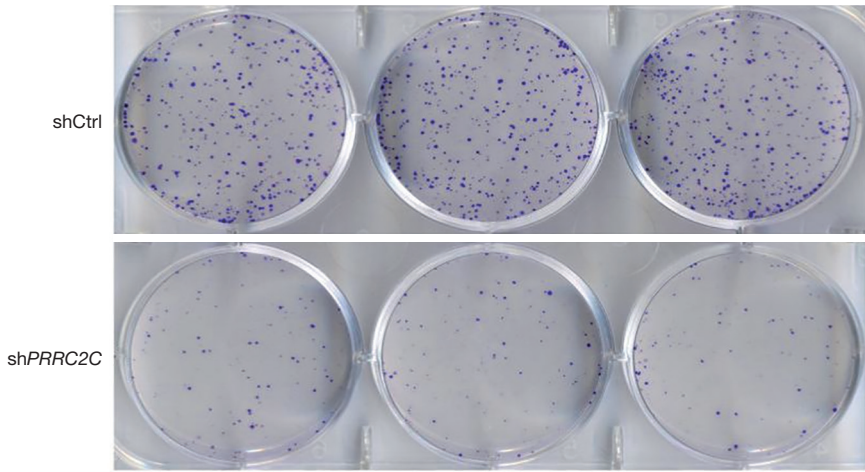


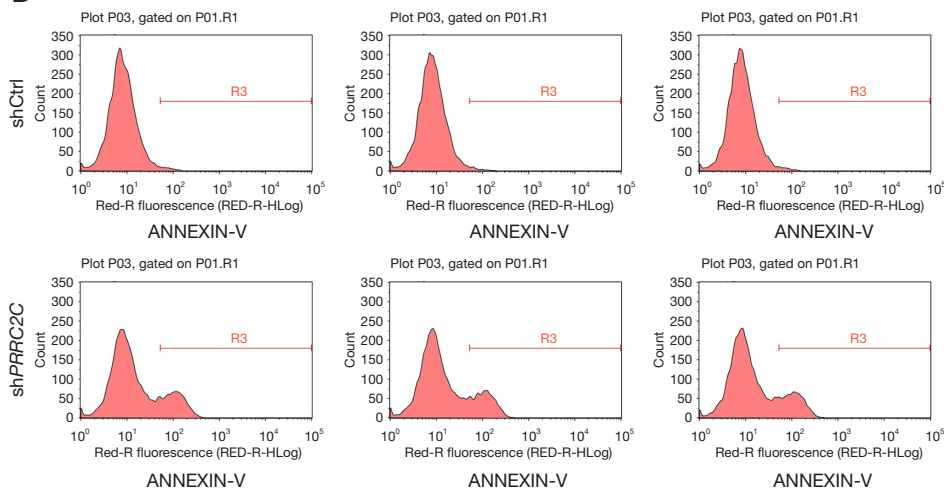
Figure 1 Correlations between proline-rich coiled-coil 2C (*PRRC2C*) expression with LIHC (liver hepatocellular carcinoma) staging, grade, and overall survival. RNA-sequencing datasets of 371 liver cancer samples and 50 control samples were obtained from The Cancer Genome Atlas (TCGA) database portal (<http://cancergenome.nih.gov/>). Differences in *PRRC2C* expression levels were analyzed between cancer and control (A), as well as among different TNM stage (B) and pathological grades (C). The cancer samples were divided into high and low expression groups and overall survival (OS) were compared between the groups using Kaplan-Meier survival analysis (D). Real-time reverse transcription polymerase chain reaction (RT-PCR) was performed to detect *PRRC2C* mRNA levels in BEL-7402, BEL-7404, SMMC-7721, and Hep G2 cell lines (E). DNA segments containing shRNA constructs targeting *PRRC2C* (sh*PRRC2C*) or non-specific control (shCtrl) were cloned into transfer vector and then introduced into cells via lentivirus infection. The mRNA levels of *PRRC2C* were tested using RT-PCR and compared between cells infected with different shRNA constructs (F). Western blot was used to detect *PRRC2C* knockdown efficiency, representative result was shown (G). GAPDH (glyceraldehyde-3-phosphate dehydrogenase) was used as an internal control. n=3. **P<0.01. ****P<0.0001.



C



D



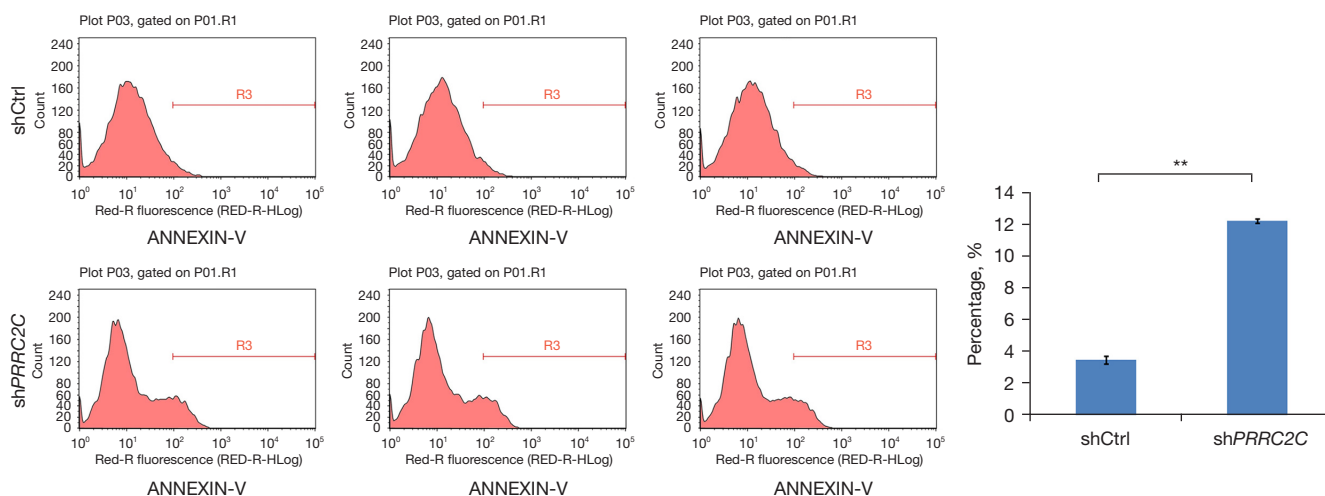


Figure 2 Proline-rich coiled-coil 2C (*PRRC2C*) knockdown inhibits cell viability/proliferation and promotes apoptosis. Viability/proliferation of cells transfected with sh*PRRC2C* or shCtrl was examined with: Celigo cell count (A), MTT assay (B), and Clone formation assay (Crystal violet staining) (C). Apoptosis of transfected cells were detected using Annexin-V and PI staining followed by flow cytometry (D). ** $P < 0.01$. MTT, 3-(4,5-dimethylthiazol-2-yl)-2,5-diphenyltetrazolium bromide.

PRRC2C silencing inhibited the migration and invasion capabilities of hepatocarcinoma cells

Using Wound healing assays, we found that the 24-h scratch migration rate in the si*PRRC2C* group was 18.38%, which was lower than that in the control group (23.13%, $P = 0.003$, Figure 3A). As expected, the number of cells that passed through Matrigel was significantly less in the experimental group than in the control group (only 51% as that of the control group, $P < 0.05$), when detected by Transwell assays (Figure 3B). Both results indicated that knocking down *PRRC2C* suppressed the cell migration and invasion of liver cancer cells.

PRRC2C regulates the tumorigenesis of liver cancer in vivo

PRRC2C silent expression cells and negative control cells were injected into nude mice and tumor development were detected in a 28-day period. As shown in Figure 4, The result showed that the *PRRC2C* silent expression group was significantly inhibited growth of tumors. In addition, the numbers of animals bearing detectable tumors at the end of experiments were also lower. Taken together, these results demonstrate that *PRRC2C* could remarkably inhibit tumorigenicity in liver cancer.

PRRC2C silencing affect expression levels of EMT signaling related genes

To determine whether regulation of liver cancer cell behavior by *PRRC2C* involves EMT, expressions of EMT-related genes were detected by RT-PCR. The expression of N-cadherin (CDH2) was significantly lower (Figure 5, $P < 0.05$), while Snail, Slug, and Smad3 was higher in the *PRRC2C* knockdown cells than that in the control group ($P < 0.05$). E-cadherin (CDH1), Twist, and Smad2/4 expression was no significantly different between the two groups ($P > 0.05$). Western blot showed that silencing *PRRC2C* inhibited the expression of N-cadherin and Vimentin.

Discussion

HCC is a complex disease due to its heterogeneity (12-14). At the molecular level, the pathogenesis of HCC includes genetic, epigenetic, and signaling pathway disorders. Meanwhile, the interaction with the tumor microenvironment leads to the occurrence, progression, and metastasis of tumors. gene amplification as a particularly common mechanism through which the expression levels of genes involved in cancer development can be regulated.

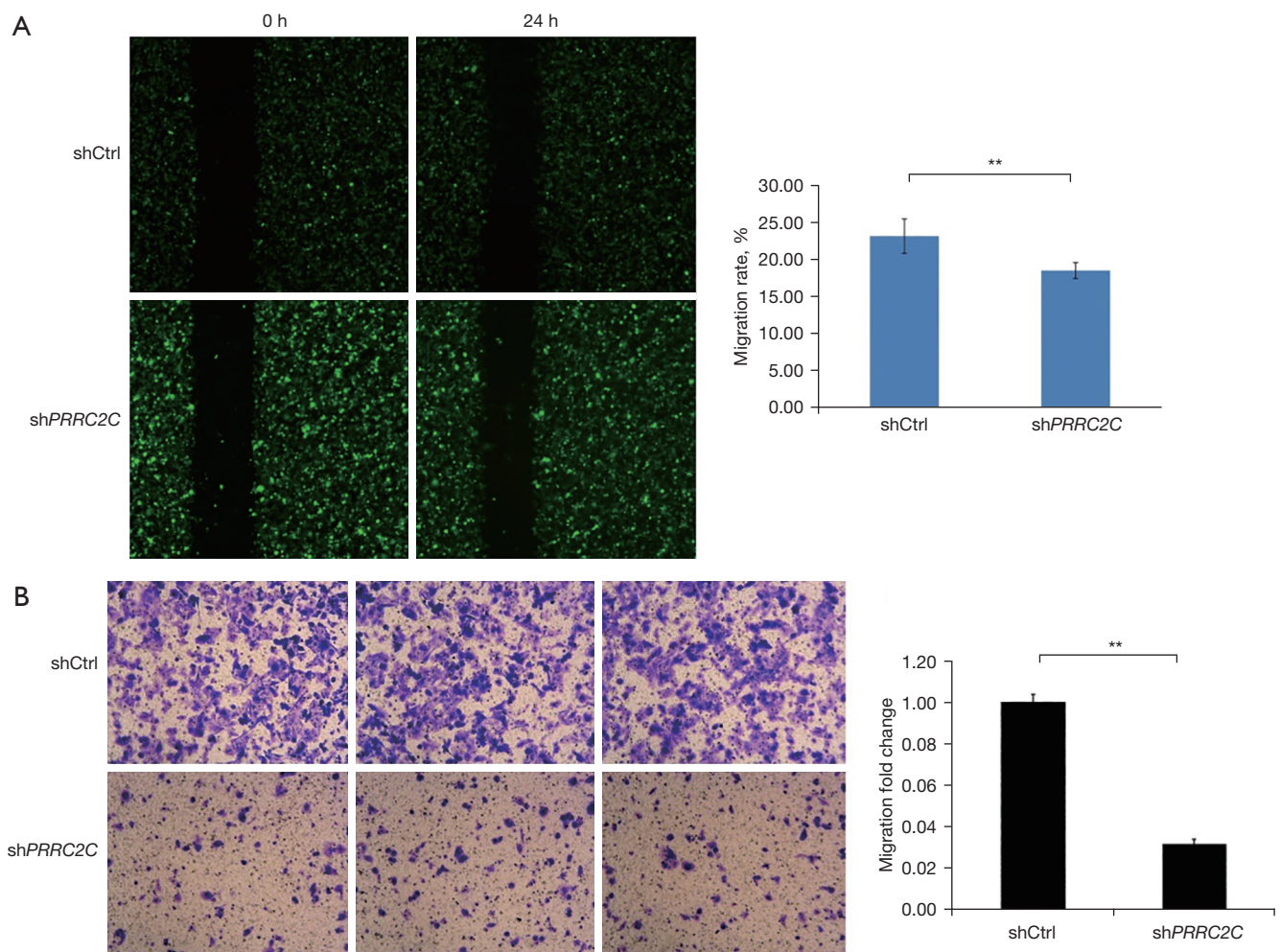
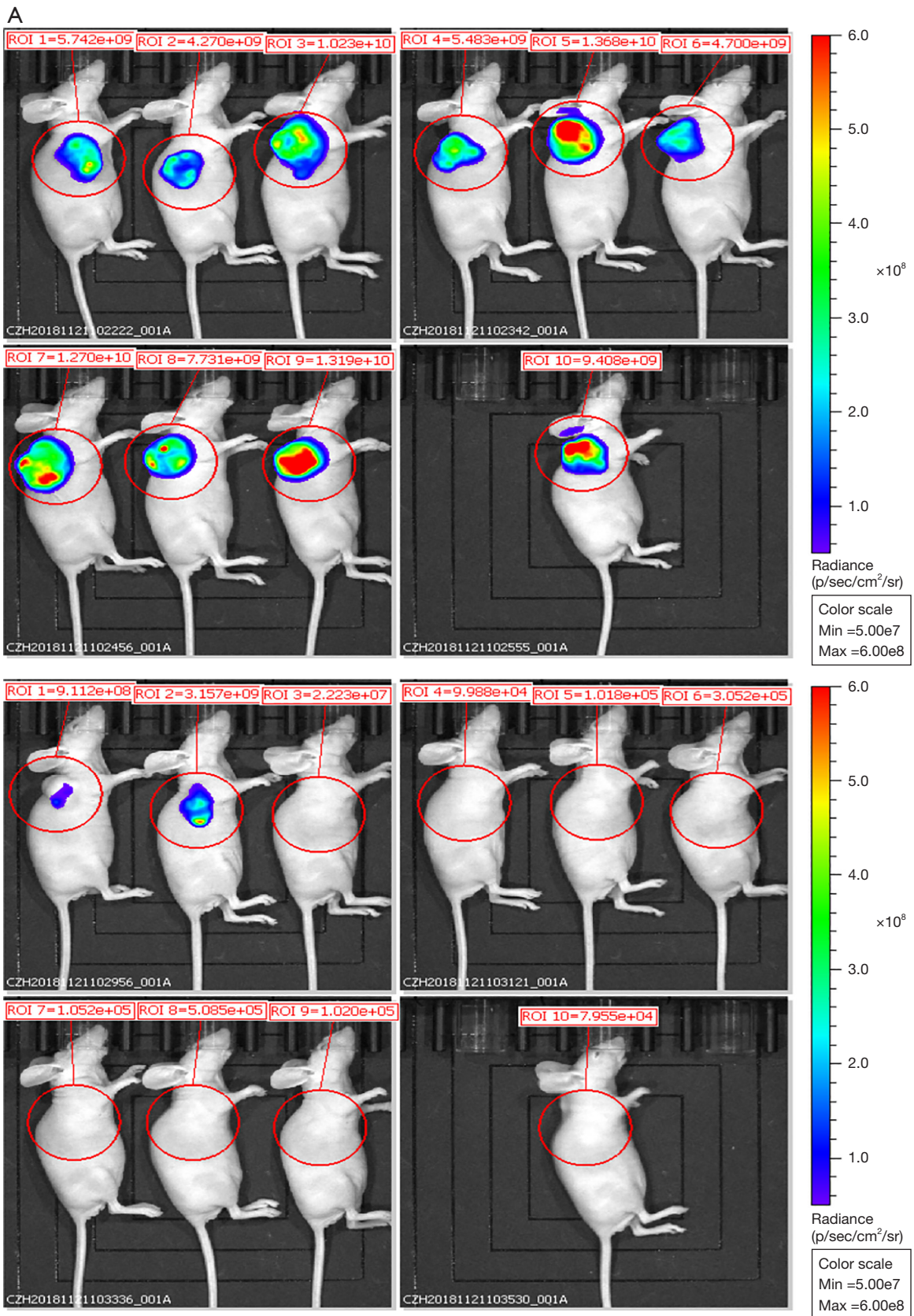


Figure 3 Proline-rich coiled-coil 2C (*PRRC2C*) knockdown inhibits cell migration and invasion. Capability of cell migration was detected using wound healing assay (100 \times) (A). Cell invasion was examined using Transwell assay (Crystal violet staining, 100 \times) (B). ** $P < 0.01$.

Gene amplification is a particularly common mechanism that regulates the increase in the number of gene copies in the genome of cancer cells, resulting in abnormal levels of gene expression in cancer development (15). In this study, *PRRC2C* was amplified and identified overexpressed in established HCC cell lines, including BEL-7402, BEL-7404, SMMC-7721 and Hep G2 cells and this result is consistent with previous studies (10,16). It also indicated that *PRRC2C* was indeed suspicious of its function in generation and development of liver cancer due to its highly expression is associated with tumor progression and poor prognosis in cancer cells.

Therefore, *PRRC2C* is distinctly ideal biological characteristics of human liver cancer.

Immortal cell proliferation and anti-apoptosis are crucial characteristics of tumors, so tumor-promoting genes generally have anti-apoptosis and pro-proliferation effects. A major finding of this study is that knockdown of *PRRC2C* could inhibit the proliferation and induce apoptosis of human hepatocarcinoma cell lines while reducing tumorigenicity of HCC cells in nude mice. It indicated that *PRRC2C* was carcinogenesis. Invasion and metastasis were also important characteristics of tumors. Since the activation of EMT has been implicated in the



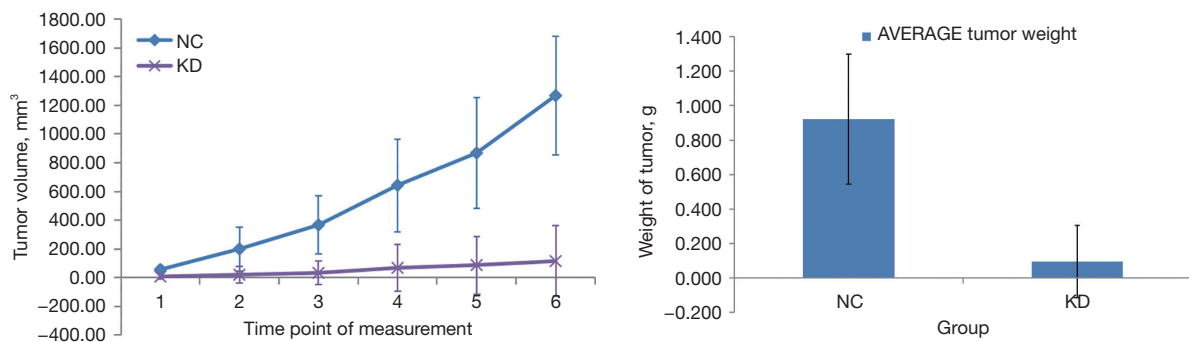
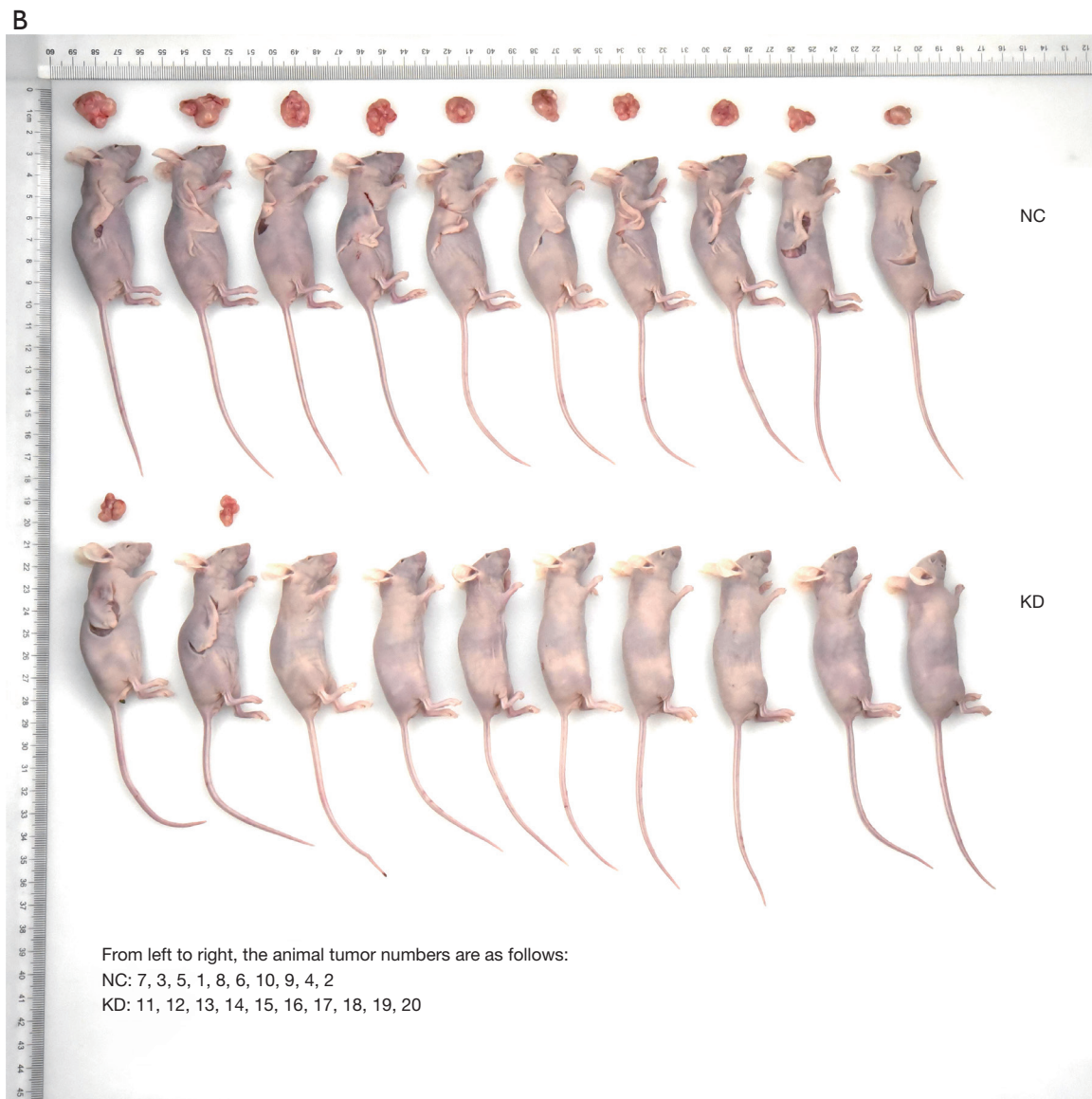
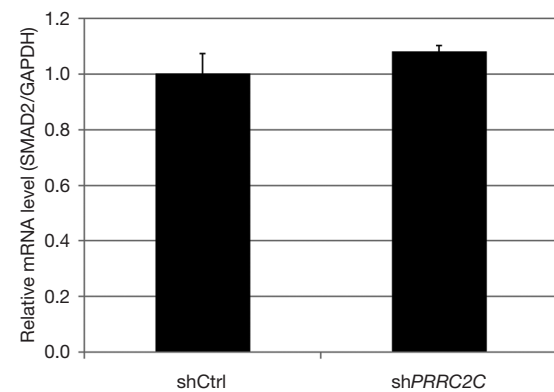
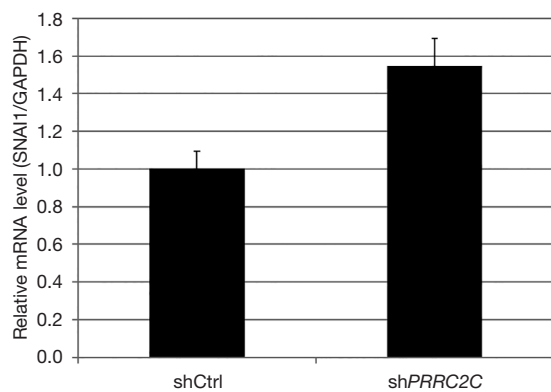
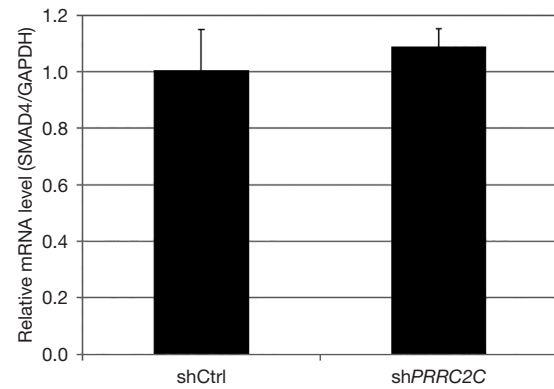
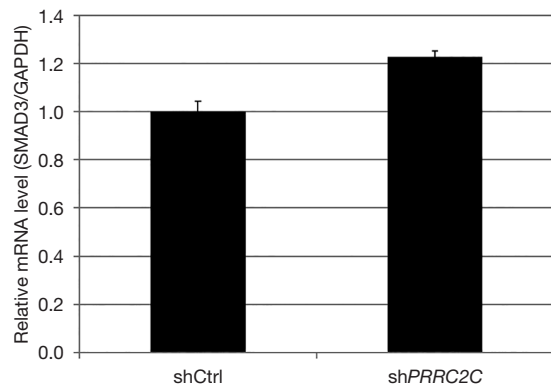
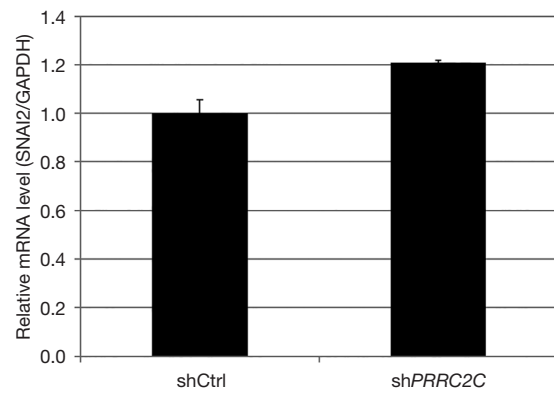
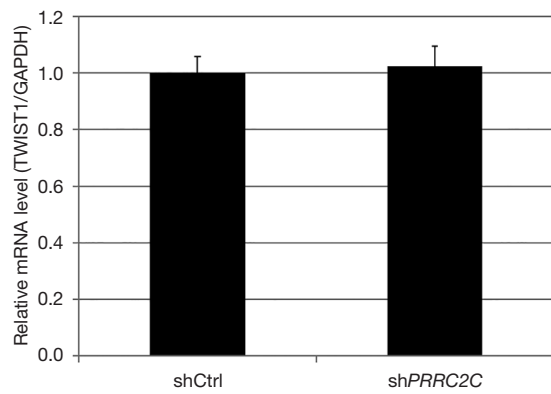
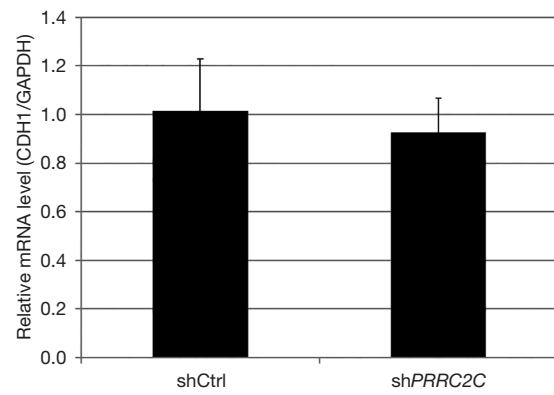
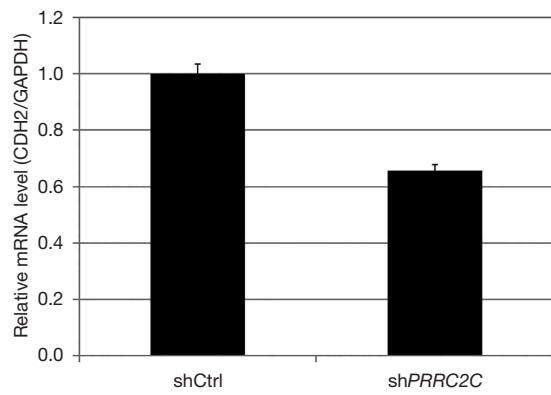


Figure 4 Proline-rich coiled-coil 2C (*PRRC2C*) knockdown inhibits tumor formation *in vivo* cells transfected with sh*PRRC2C* (KD) or shCtrl (NC) were inoculated into BALB/c nude mice to induce xenograft tumor. The growth of tumor was monitored by fluorescence detection (A). Tumors were isolated from experimental animals at different time points. Sizes and growth rate were quantified and compared between cells transfected with shCtrl and sh*PRRC2C* constructs (B).



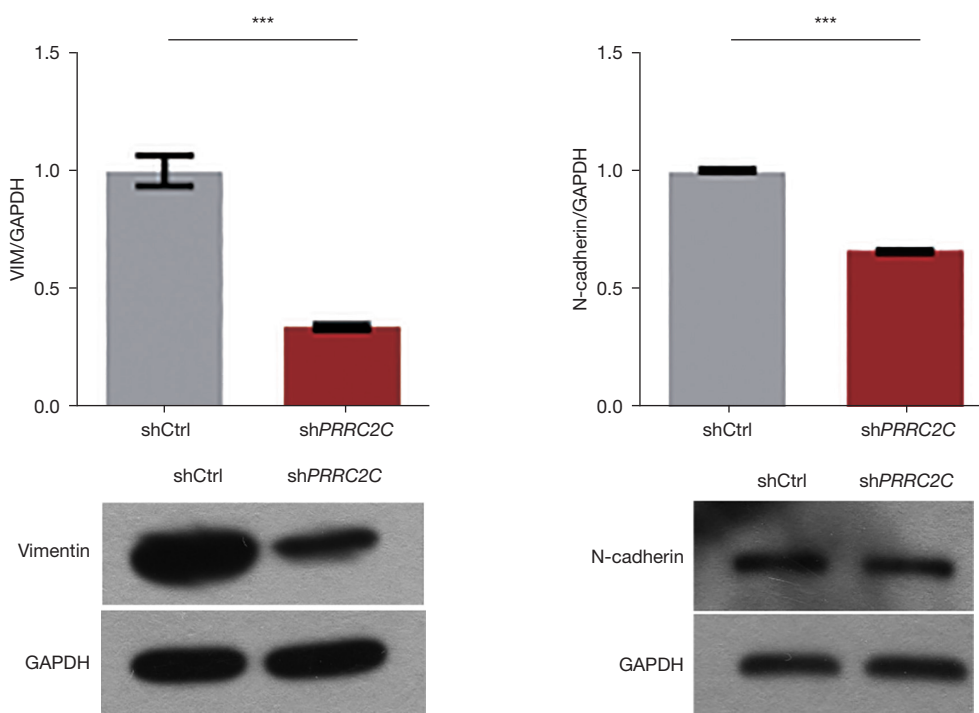


Figure 5 Effects of proline-rich coiled-coil 2C (*PRRC2C*) knockdown on EMT related gene expression. RT-PCR was used to detect the mRNA levels of genes coding N-cadherin (*CDH2*), E-cadherin (*CDH1*), *TWIST1*, *SMAD2/3/4* and *SNAI1/2*. Vimentin and N-cadherin were detected by Western blotting. *** $P < 0.001$. **** $P < 0.0001$. RT-PCR, reverse transcription-polymerase chain reaction.

metastasis of human tumors, we observed that knockdown of *PRRC2C* profoundly suppressed the invasion of liver cancer cells and the EMT-related gene N-cadherin in this study, but our results did not clarify which pathway through which *PRRC2C* may regulate E-cadherin, because various transcription factors have been reported to regulate E-cadherin expression. It only suggested that *PRRC2C* may involve in tumor progression. In addition, EMT process depends on the changes in the expression levels of dozens or even hundreds of genes. The exact mechanism that *PRRC2C* was involved in this process needs further investigation.

Very few studies have been carried out on *PRRC2C* leading that the specific molecular mechanism of *PRRC2C* is still unclear. As a proline-rich protein, its possible mechanism is often taking interaction with other proteins. *PRRC2C* has been suggested to be associate with stress granules (4) and may be involved in epigenetic regulation of gene expression in stress conditions, while the expression of *PRRC2C* may be regulated at splicing level. The evidence from a primary non-small cell lung cancer proved that *SRSF1* overexpression led to abnormal splicing of

PRRC2C two alternative spliced products *PRRC2C-L* (long) and *PRRC2C-S* (short), then knock down *PRRC2C-L* and *PRRC2C-S* reduced proliferation of lung cancer A549 cells (7). These results indicated that the abnormal splicing of *PRRC2C* was involved in the carcinogenic process and regulated by *SRSF1*, which belongs to the serine/arginine-rich protein family and is involved in several human tumors (17-19).

Conclusions

The conclusion from this study indicated that *PRRC2C* promotes the proliferation and metastasis of liver cancer cells and potentially involved in EMT related genes expression.

Acknowledgments

Funding: The study was supported by Shaoguan City Science and Technology Plan Project [grant number 200812114531509]; and Shaoguan City Health Research Project [grant number Y20203].

Footnote

Reporting Checklist: The authors have completed the ARRIVE reporting checklist. Available at <https://jgo.amegroups.com/article/view/10.21037/jgo-23-10/rc>

Data Sharing Statement: Available at <https://jgo.amegroups.com/article/view/10.21037/jgo-23-10/dss>

Conflicts of Interest: All authors have completed the ICMJE uniform disclosure form (available at <https://jgo.amegroups.com/article/view/10.21037/jgo-23-10/coif>). The authors have no conflicts of interest to declare.

Ethical Statement: The authors are accountable for all aspects of the work in ensuring that questions related to the accuracy or integrity of any part of the work are appropriately investigated and resolved. The study was conducted in accordance with the Declaration of Helsinki (as revised in 2013). Animal experiments were performed under a project license (No. SUMC2019-355) granted by the Medical Animal Care & Welfare Committee of Shantou University Medical College, in compliance with the Shantou University guidelines for the care and use of animals.

Open Access Statement: This is an Open Access article distributed in accordance with the Creative Commons Attribution-NonCommercial-NoDerivs 4.0 International License (CC BY-NC-ND 4.0), which permits the non-commercial replication and distribution of the article with the strict proviso that no changes or edits are made and the original work is properly cited (including links to both the formal publication through the relevant DOI and the license). See: <https://creativecommons.org/licenses/by-nc-nd/4.0/>.

References

1. Bray F, Ferlay J, Soerjomataram I, et al. Global cancer statistics 2018: GLOBOCAN estimates of incidence and mortality worldwide for 36 cancers in 185 countries. *CA Cancer J Clin* 2018;68:394-424.
2. Siegel R, Naishadham D, Jemal A. Cancer statistics, 2013. *CA Cancer J Clin* 2013;63:11-30.
3. Nie J, Lu L, Du C, et al. FAM83D promotes the proliferation and migration of hepatocellular carcinoma cells by inhibiting the FBXW7/MCL1 pathway. *Transl Cancer Res* 2022;11:3790-802.
4. Youn JY, Dunham WH, Hong SJ, et al. High-Density Proximity Mapping Reveals the Subcellular Organization of mRNA-Associated Granules and Bodies. *Mol Cell* 2018;69:517-532.e11.
5. Kikuno R, Nagase T, Ishikawa K, et al. Prediction of the coding sequences of unidentified human genes. XIV. The complete sequences of 100 new cDNA clones from brain which code for large proteins in vitro. *DNA Res* 1999;6:197-205.
6. Huang WC, Taylor S, Nguyen TB, et al. KIAA1096, a gene on chromosome 1q, is amplified and overexpressed in bladder cancer. *DNA Cell Biol* 2002;21:707-15.
7. de Miguel FJ, Sharma RD, Pajares MJ, et al. Identification of alternative splicing events regulated by the oncogenic factor SRSF1 in lung cancer. *Cancer Res* 2014;74:1105-15.
8. Kaymaz Y, Oduor CI, Yu H, et al. Comprehensive Transcriptome and Mutational Profiling of Endemic Burkitt Lymphoma Reveals EBV Type-Specific Differences. *Mol Cancer Res* 2017;15:563-76.
9. Jacobo-Baca G, Salazar-Ybarra RA, Torres-de-la-Cruz V, et al. Proteomic profile of preeclampsia in the first trimester of pregnancy. *J Matern Fetal Neonatal Med* 2022;35:3446-52.
10. Kim HE, Kim DG, Lee KJ, et al. Frequent amplification of CENPF, GMNN and CDK13 genes in hepatocellular carcinomas. *PLoS One* 2012;7:e43223.
11. Sang Y, Chen B, Song X, et al. circRNA_0025202 Regulates Tamoxifen Sensitivity and Tumor Progression via Regulating the miR-182-5p/FOXO3a Axis in Breast Cancer. *Mol Ther* 2019;27:1638-52.
12. Ferlay J, Soerjomataram I, Dikshit R, et al. Cancer incidence and mortality worldwide: sources, methods and major patterns in GLOBOCAN 2012. *Int J Cancer* 2015;136:E359-86.
13. Khalaf N, Ying J, Mittal S, et al. Natural History of Untreated Hepatocellular Carcinoma in a US Cohort and the Role of Cancer Surveillance. *Clin Gastroenterol Hepatol* 2017;15:273-281.e1.
14. Dhanasekaran R, Bandoh S, Roberts LR. Molecular pathogenesis of hepatocellular carcinoma and impact of therapeutic advances. *F1000Res* 2016;5:F1000 Faculty Rev-879.
15. Medina PP, Castillo SD, Blanco S, et al. The SRY-HMG box gene, SOX4, is a target of gene amplification at chromosome 6p in lung cancer. *Hum Mol Genet* 2009;18:1343-52.
16. Nong YX, Huang JL, Huang ZS, et al. Characteristics

- and experimental applications of human hepatocellular carcinoma cell lines. *World Chinese Journal of Digestology* 2017;25:159.
17. Long JC, Caceres JF. The SR protein family of splicing factors: master regulators of gene expression. *Biochem J* 2009;417:15-27.
 18. Shen S, Warzecha CC, Carstens RP, et al. MADS+: discovery of differential splicing events from Affymetrix exon junction array data. *Bioinformatics* 2010;26:268-9.
 19. Kechris K, Yang YH, Yeh RF. Prediction of alternatively skipped exons and splicing enhancers from exon junction arrays. *BMC Genomics* 2008;9:551.

Cite this article as: Zhang K, Xu J, Chen R. Silencing proline-rich coiled-coil 2C inhibit the proliferation and metastasis of liver cancer cells. *J Gastrointest Oncol* 2023;14(1):287-301. doi: 10.21037/jgo-23-10